

## Temperature modulation molecularbeam epitaxy and its application to the growth of periodic index separate confinement heterostructure InGaAs quantumwell lasers

M. Hong, M. C. Wu, Y. K. Chen, J. P. Mannaerts, and M. A. Chin

Citation: *Journal of Vacuum Science & Technology B* **10**, 989 (1992); doi: 10.1116/1.586109

View online: <http://dx.doi.org/10.1116/1.586109>

View Table of Contents: <http://scitation.aip.org/content/avs/journal/jvstb/10/2?ver=pdfcov>

Published by the AVS: Science & Technology of Materials, Interfaces, and Processing

### Articles you may be interested in

Periodic index separate confinement heterostructure InGaAs/AlGaAs quantum well lasers grown by temperature modulation molecular beam epitaxy

Appl. Phys. Lett. **61**, 43 (1992); 10.1063/1.107662

Effects of substrate heating on the spatial uniformity of threshold current and emission wavelength in GaAs and InGaAs gradedindex separateconfinement heterostructure quantumwell lasers grown by molecularbeam epitaxy

J. Vac. Sci. Technol. B **10**, 1006 (1992); 10.1116/1.586399

Periodic index separate confinement heterostructure InGaAs/AlGaAs multiple quantum well laser grown by organometallic vapor phase epitaxy


Appl. Phys. Lett. **60**, 598 (1992); 10.1063/1.106565

Strainedlayer InGaAsGaAsAlGaAs gradedindex separate confinement heterostructure single quantum well lasers grown by molecular beam epitaxy

Appl. Phys. Lett. **54**, 2527 (1989); 10.1063/1.101083

Lowthreshold interruptedgrowth stepindex separateconfinement heterostructure GaAs/(Al,Ga)As lasers grown by molecularbeam epitaxy

J. Appl. Phys. **63**, 588 (1988); 10.1063/1.340096



## Instruments for Advanced Science

<p>Contact Hiden Analytical for further details:  <b>W</b> <a href="http://www.HidenAnalytical.com">www.HidenAnalytical.com</a>  <b>E</b> <a href="mailto:info@hiden.co.uk">info@hiden.co.uk</a></p> <p><b>CLICK TO VIEW</b> our product catalogue</p>	 <p><b>Gas Analysis</b></p> <ul style="list-style-type: none"> <li>› dynamic measurement of reaction gas streams</li> <li>› catalysis and thermal analysis</li> <li>› molecular beam studies</li> <li>› dissolved species probes</li> <li>› fermentation, environmental and ecological studies</li> </ul>	 <p><b>Surface Science</b></p> <ul style="list-style-type: none"> <li>› UHV TPD</li> <li>› SIMS</li> <li>› end point detection in ion beam etch</li> <li>› elemental imaging - surface mapping</li> </ul>	 <p><b>Plasma Diagnostics</b></p> <ul style="list-style-type: none"> <li>› plasma source characterization</li> <li>› etch and deposition process reaction</li> <li>› kinetic studies</li> <li>› analysis of neutral and radical species</li> </ul>	 <p><b>Vacuum Analysis</b></p> <ul style="list-style-type: none"> <li>› partial pressure measurement and control of process gases</li> <li>› reactive sputter process control</li> <li>› vacuum diagnostics</li> <li>› vacuum coating process monitoring</li> </ul>
--	--	--	--	--

# Temperature modulation molecular-beam epitaxy and its application to the growth of periodic index separate confinement heterostructure InGaAs quantum-well lasers

M. Hong, M. C. Wu, Y. K. Chen, J. P. Mannaerts, and M. A. Chin  
AT&T Bell Laboratories, Murray Hill, New Jersey 07974

(Received 16 September 1991; accepted 29 October 1991)

Solid-source molecular-beam epitaxy has been employed to grow periodic index separate confinement heterostructure InGaAs quantum-well lasers emitting at 980 nm. The  $5\ \mu\text{m} \times 750\ \mu\text{m}$  device fabricated using a self-aligned process has far-field angles of  $10^\circ$  by  $20^\circ$ , a threshold current of 45 mA, an external differential quantum efficiency of 1.15 mW/mA (90%), and an output power of 620 mW, all measured at room temperature under cw operation. A record high fiber coupling efficiency of 51% has been achieved.

## I. INTRODUCTION

High power semiconductor lasers with small circular optical beam divergence find applications in fiber optics,<sup>1</sup> optical data storages, and free-space optical interconnects. Lasers using a conventional graded-index separate confinement heterostructure (GRINSCH) have produced low threshold currents and high quantum efficiencies. However, the tight optical confinement of the GRINSCH structure generates large beam divergence in the direction perpendicular to the junction plane ( $\sim 50^\circ$  for InGaAs/AlGaAs lasers).<sup>1</sup> This then gives a highly elliptical far-field pattern, and consequently, results in low efficiency in light collection. The beam divergence can be reduced by expanding the transverse mode size in the laser cavity.<sup>2-4</sup> A new quantum-well (QW) laser in a configuration of periodic index separate confinement heterostructure (PINSCH) has been demonstrated to achieve this goal.<sup>4</sup>

The PINSCH laser utilizes the periodic-index (PIN) confining layers to expand the optical mode size and to achieve the electrical carrier confinement at the same time. The transverse beam in the PINSCH laser is reduced to  $20^\circ$ , along with attainment of a high output power exceeding 620 mW. The laser was grown using a novel temperature modulation molecular-beam epitaxy (MBE).<sup>5</sup> In this article, detailed growth parameters on the new-technique, and a comparison between our technique and conventional approaches are discussed. We then briefly explain the concept of the PINSCH laser and finally present the characteristics of this new laser.

## II. TEMPERATURE MODULATION MBE

One difference between GRINSCH and PINSCH lasers shown in Fig. 1 is that the latter utilizes several pairs of GaAs/AlGaAs multilayers on each side of the active region to expand the optical field. A precise control (within 5%–10%) of the layer thickness and composition is required for the growth of the PINSCH structure. Also, large barrier heights formed at the heterointerface between GaAs and AlGaAs due to the energy band gap difference between the two constituents may impede the carrier flow and give large series resistance. In the area of high output power, the series resistance in the multilayers causes ther-

mal heating and deteriorates the laser performance. For GaAs/Al<sub>0.4</sub>Ga<sub>0.6</sub>As with a sharp interface [Fig. 2(a)], a calculated valence band diagram with a *p*-type doping level of  $5 \times 10^{17}\ \text{cm}^{-3}$  is shown in Fig. 2(c). The calculation was obtained using the Fermi-Dirac statistics, and a self-consistent method to solve the Poisson equation.<sup>6</sup> The barrier height for the holes from GaAs to Al<sub>0.4</sub>Ga<sub>0.6</sub>As is 260 meV, which is much greater than the thermal energy of 25 meV at room temperature.

In this work, the barrier height has been reduced by continuously grading the interface of GaAs/Al<sub>0.4</sub>Ga<sub>0.6</sub>As. Experimentally, this is accomplished by simultaneously varying cell temperatures of Al and Ga without any shutter operation. For GaAs/Al<sub>0.4</sub>Ga<sub>0.6</sub>As with a linearly graded interface of 500 Å [Fig. 2(b)], a calculated valence band diagram for a *p* doping of  $5 \times 10^{17}\ \text{cm}^{-3}$  is shown in Fig. 2(c). The large energy barrier of 260 meV for the sharp interface of GaAs and Al<sub>0.4</sub>Ga<sub>0.6</sub>As has been greatly reduced to 22 meV in the case of linearly graded interfaces for the same level of *p* or *n* doping. As a consequence, low resistance has been achieved without employing a high doping at the heterointerfaces, which increases the cavity loss due to free-carrier absorption.

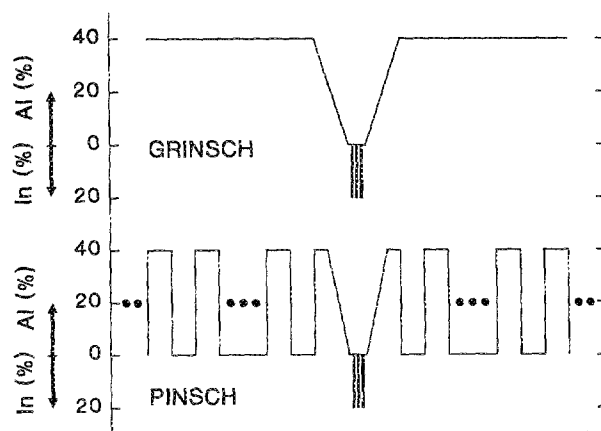


FIG. 1. Schematics of GRINSCH and PINSCH QW lasers. Only a few pairs of AlGaAs/GaAs are needed for the PINSCH confining layers.

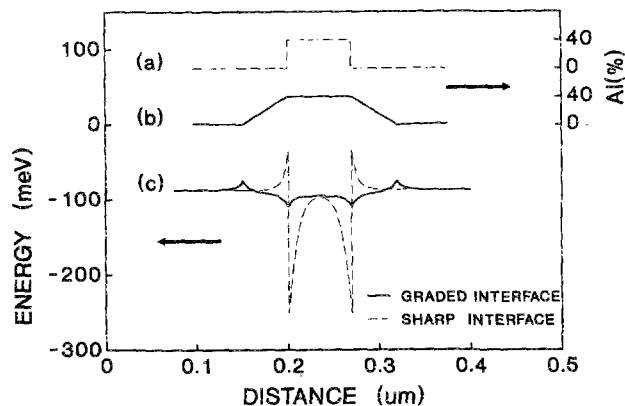


FIG. 2. Schematics of GaAs/Al<sub>0.4</sub>Ga<sub>0.6</sub>As with sharp (a) and linearly graded (b) interfaces. Calculated valence band diagrams (Ref. 6) for (a) and (b) are shown in (c).

The nominal doping levels in the PINSCH structure are  $0.2\text{--}1.0 \times 10^{18} \text{ cm}^{-3}$  for the *n* type and  $1.0 \times 10^{18} \text{ cm}^{-3}$  for the *p* type. The active region and the adjacent 500 Å in the confinement layers are undoped. The doping levels are similar to those of conventional GRINSCH lasers. A series resistance as small as 2 Ω is achieved for a  $4 \mu\text{m} \times 750 \mu\text{m}$  PINSCH laser. This value is no different than those obtained in the GRINSCH lasers.

During the growth of the PIN layers, the shutters for Ga and Al are kept open. In other words, the fluxes of Ga and Al are controlled *only* by the cell temperatures, which are computer-programmed to grow GaAs, AlGaAs, and the interfaces. The computer programming of the cell temperatures is based on accurate growth rates of GaAs, AlAs, and AlGaAs carefully calibrated using reflection high-energy electron diffraction (RHEED) oscillations, flux gauge measurement near the substrate, optical reflectivity measurements, and high resolution x-ray diffraction.

Using our new shutterless temperature modulation MBE, the growth rates for GaAs, Al<sub>0.4</sub>Ga<sub>0.6</sub>As, and the graded area are kept constant. This makes it easy in producing desirable doping profiles and in keeping minimal As overpressure necessary for good growth of GaAs and AlGaAs. In comparison, for growing conventional GaAs/AlGaAs multilayers, cell temperatures of Ga and Al remain constant, and the fluxes of Ga and Al are controlled only by the shutter operation. It is difficult to keep constant growth rates using the conventional method for growing the multilayers with interfaces having one or two layers of intermediate compositions.

The substrate temperature was kept constant at 600 °C for precise control of the layer thickness and composition even for the growth of Al<sub>0.4</sub>Ga<sub>0.6</sub>As. The substrate temperature was then gradually lowered to 550–560 °C for the growth of the active region including In<sub>0.2</sub>Ga<sub>0.8</sub>As. This growth condition has consistently given the PINSCH structure lasing at 980 nm.

### III. DEVICE AND CHARACTERISTICS OF PINSCH LASER

A typical PINSCH laser for emitting at 980 nm is schematically shown in Fig. 1, which consists of three parts: an

active region in the center and PIN confinement layers on either side of the active region. The active region comprises three In<sub>0.2</sub>Ga<sub>0.8</sub>As quantum wells 70 Å thick and four GaAs barriers 200 Å thick. Each PIN confinement layer consists of eight pairs of Al<sub>0.4</sub>Ga<sub>0.6</sub>As/GaAs periodic multilayers. The laser can also be designed to emit other wavelengths.

The advantages of the PINSCH laser are that the transverse optical mode profile can be independently synthesized and expanded, while the electrical carrier confinement is as good as that of the GRINSCH structure. Synthesis of the transverse mode size is carried out by adjusting the layer thicknesses of the periodic media. Moreover, all the high-order transverse modes are totally suppressed in the PINSCH structure. The suppression of high-order spatial modes is very important for applications which require diffraction-limited beam profile and high efficiency in light collection. In actual implementation of the PINSCH lasers, only a finite number of PIN layers are needed because the optical field decays quickly within a couple of periods.

Ridge-waveguide PINSCH lasers are fabricated using a previously reported self-aligned process.<sup>8</sup> A ridge waveguide 4–5 μm wide is formed by wet chemical etching and planarized by polyimide. The thickness of the remaining cladding layer above the active quantum wells is 0.45 μm, about one pair of AlGaAs/GaAs PIN confinement layers. Though higher threshold current densities than that of the GRINSCH lasers are expected because of the lower optical confinement factors, a value of 500 A/cm<sup>2</sup> from the broad area laser is achieved.

The transverse mode is guided by the PINSCH structure, and the lateral mode is index-guided by the ridge waveguide. Single transverse-mode operation with full width at half-maximum far-field angles of  $\theta_{\parallel} = 20^{\circ}$  is observed for all output power levels. On the other hand, single lateral mode operation with  $\theta_{\perp} = 9.4^{\circ}$  is obtained only up to 150 mW. The  $\theta_{\perp}/\theta_{\parallel}$  ratio is 2.1, about two to three times better than that of the InGaAs/AlGaAs GRINSCH lasers. The far-field patterns for typical GRINSCH and PINSCH lasers are shown in Fig. 3.

The room-temperature continuous wave (cw) light-versus-current (*L-I*) curve of a self-aligned ridge-waveguide PINSCH laser 750 μm long is shown in Fig. 4. The reflectivities of the front and back facets are about 10% and 90%, respectively, after coatings. A threshold current of 45 mA and an external differential quantum efficiency of 1.15 mW/mA (90%) are achieved. The cw output power into free space exceeds 620 mW at a pump current of 700 mA. Normalizing the power with the width of the laser, the maximum output power is 120 mW/μm, the highest value ever reported for ridge-waveguide strained-layer InGaAs QW lasers. The more symmetric beam profile greatly increases the optical coupling efficiency into optical fibers. A coupling efficiency of 51% is obtained and more than 130 mW of power is coupled into a 5 μm-core single mode fiber.

The  $\Gamma$  factor in the PINSCH is approximately 1/2.5 of that of the GRINSCH with an identical active structure.

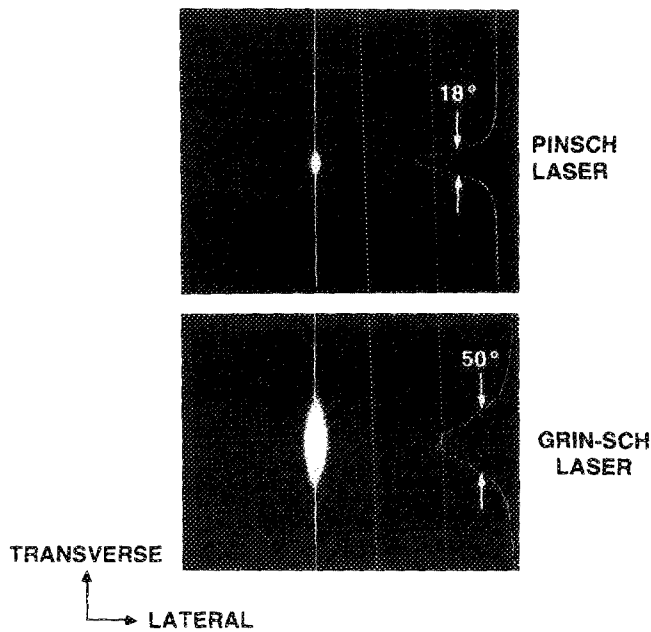
4  $\mu\text{m}$  WIDE SAL RIDGE WAVEGUIDE LASERS

FIG. 3. Far-field patterns of GRINSCH and PINSCH lasers.

As a result,  $J_{th}$  will increase by about the same factor (2.5) for the same cavity length. However, the quantum efficiency  $\eta$  is better than or equal to that of GRINSCH, because of the smaller internal loss.

#### IV. CONCLUSION

Solid-source MBE with an ability of modulating cell temperatures has been fine tuned to grow the PINSCH structure. In particular, the PIN multilayers were grown without any shutter operation. The PINSCH structure expands the fundamental transverse mode size while totally suppressing the high-order modes and efficiently confining

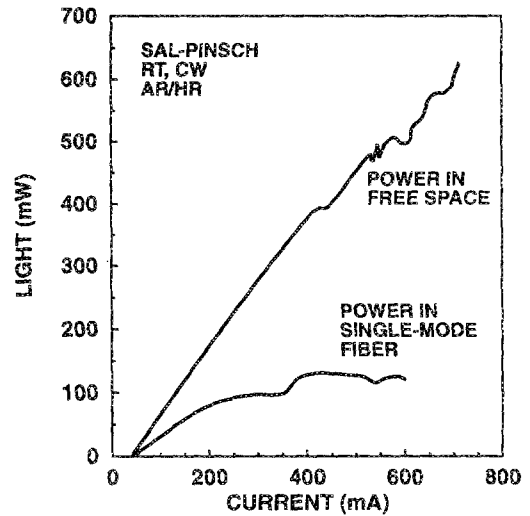


FIG. 4. Room-temperature cw  $L$ - $I$  curves of a  $5 \mu\text{m} \times 750 \mu\text{m}$  PINSCH laser showing output power in free space and coupled into a single mode fiber with  $5 \mu\text{m}$  core diameter (Ref. 4). The maximum output powers in free space and in the fiber are 620 and 130 mW, respectively. The output power of 620 mW is thermally limited.

the injected electrical carriers. A high power laser and a record high coupling efficiency into single mode fiber are achieved.

- <sup>1</sup>S. Uehara, M. Okayasu, T. Takeshita, O. Kogure, M. Yamada, M. Shimizu, and M. Horiguchi, *Optoelectronics* **5**, 71 (1990).
- <sup>2</sup>H. F. Lockwood, H. Kressel, H. S. Sommers, and F. Z. Hawrylo, *Appl. Phys. Lett.* **17**, 499 (1970).
- <sup>3</sup>Y. C. Chen, R. G. Waters, and R. J. Dalby, *Electron. Lett.* **26**, 1348 (1990).
- <sup>4</sup>M. C. Wu, Y. K. Chen, M. Hong, J. P. Mannaerts, M. A. Chin, and A. M. Sergent, *Appl. Phys. Lett.* **59**, 1046 (1991).
- <sup>5</sup>M. Hong, J. P. Mannaerts, J. H. Hong, R. J. Fischer, K. Tai, J. Kwo, J. M. Vandenberg, Y. H. Wang, and J. Gamelin, *J. Cryst. Growth* **11**, 1071 (1991).
- <sup>6</sup>J. Gamelin and J. H. Hong (private communication).
- <sup>7</sup>H. Kogelnik and C. V. Shank, *J. Appl. Phys.* **43**, 2328 (1972).
- <sup>8</sup>Y. K. Chen, M. C. Wu, W. S. Hobson, S. J. Pearton, A. M. Sergent, and M. A. Chin, *IEEE Photonics Tech. Lett.* **3**, 408 (1991).